Soriano-Amat, M., Marcon, L., Costa, L., García-Ruiz, A., Martins, H. F., Martín-López, S., Palmieri, L. & González-Herráez, M. 2019, "Characterization and modelling of induced virtual perturbations in chirped pulse φOTDR", Proceedings of SPIE, vol. 11199, 7th European Workshop on Optical Fibre Sensors, 111992A

Available at http://dx.doi.org/10.1117/12.2540760

(Article begins on next page)

Characterization and modelling of induced "virtual" perturbations in chirped pulse φ-OTDR

Miguel Soriano-Amat[*,a], Leonardo Marcon[b], Luis Costa[a], Andres Garcia-Ruiz[a], Hugo F. Martins[c], Sonia Martin-Lopez[a], Luca Palmieri[b], and Miguel Gonzalez-Herraez[a]
[a] Departamento de Electrónica, Universidad de Alcalá, Edificio Politecnico, Madrid 28871, Spain
[b] Department of Information Engineering - University of Padova, Via G. Gradenigo 6/B, 35131 Padova (PD), Italy
[c]Instituto de Óptica "Daza de Valdés", IO-CSIC, C/Serrano 121, Madrid 28006, Spain

ABSTRACT

Any temperature change or strain acting on a section of the fiber induces a local variation of the refractive index. If the fiber is monitored by a chirped pulse φ-OTDR system, the variation of the refractive index causes a local shift of the backscattering trace and produces a change in the round trip time of the light coming from any further position of the fiber. While usually negligible, due to the high sensitivity of the chirped pulse φ-OTDR, in extreme occasions the distributed round trip time change may appear in the measurement as an undesired "virtual" perturbation. In this paper, we discuss and experimentally validate a mathematical model to account for (and eventually correct) the "virtual" perturbation.

Keywords: Phase-sensitive OTDR, Rayleigh scattering, Distributed Acoustic Sensing.

1. INTRODUCTION

Optical fiber scattering phenomena, namely Rayleigh, Brillouin or Raman, allow the realization of high performance distributed sensors[1]. The easiest phenomenon to exploit is Rayleigh backscattering, generated by the local inhomogeneity of the fiber refractive index, which is extremely sensitive to environmental perturbations like temperature changes or vibrations[2]. A common setup used to realize distributed acoustic sensors (DAS) based on Rayleigh backscattering is the phase-sensitive optical time domain reflectometer (φ-OTDR)[3]. This technique uses a coherent laser source to interrogate tens of kilometers of fiber with spatial resolution of meters and acoustic bandwidth of kilohertz. To improve the performance of φ-OTDR setups and partially mitigate its issues, (like coherent fading), a setup called chirped pulse φ-OTDR has been reported recently[4]. In this setup, the traditional flat-phase input pulse is replaced with a linearly chirped one, transforming the measurement procedure into a time-delay estimation process. This increases the robustness of the setup, allowing to reach sensitivities of mK or nε. However, the time delay estimation procedure may cause some impact since a very large perturbation acting on a section of fiber may cause a variation in the local refractive index that is translated into a certain delay there onwards in the measured trace. In other words, the perturbation induces a distortion in the round trip time of all the backscattering components generated beyond the stressed section of the fiber. This distortion, which can be considered negligible in the vast majority of the cases, may become significant if the variation of the refractive index is very large. This is unlikely to happen in the usual applications of monitoring of long perimeters or pipelines[5,6], but may happen if long sections of the fiber experience a uniform and large environmental perturbation. In this paper, we discuss and validate experimentally a mathematical model for the perturbation-induced round trip time change that appears, in the measurement performed with a chirped pulse φ-OTDR, as a virtual perturbation. The experiment is performed by inducing a fairly large temperature change over a known section of the fiber and by monitoring a further fiber section kept at rest. The proposed model could be used by an algorithm to estimate the virtual perturbations induced by all the real stresses acting on fiber and progressively remove them.

2. THEORETICAL MODEL

As the input pulse of a chirped pulse φ-OTDR $P(t, z)$, of width τ_p, central frequency υ_0 and total applied chirp $\delta\upsilon$, propagates along the fiber, a small part of its power $B(t)$ gets back-reflected due to Rayleigh scattering. The round trip

* miguel.soriano@uah.es

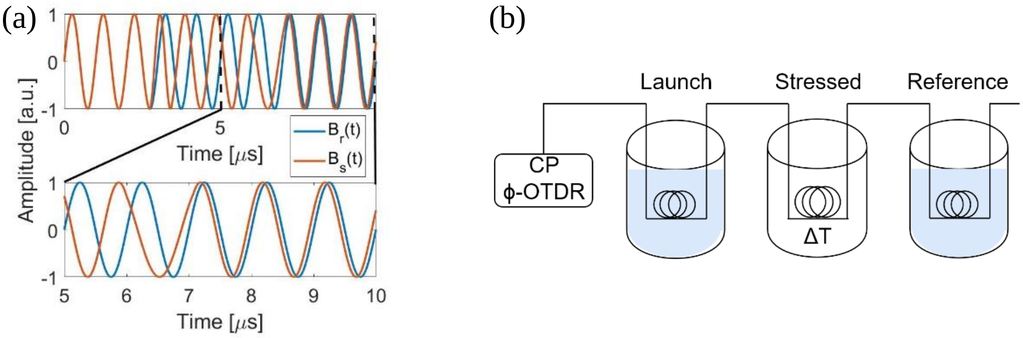

Figure 1. (a) Consequences of a localized stress on a simplified $B(t)$. On the bottom a zoom of the traces after the perturbation. (b) Schematic representation of the setup.

time of the light in the fiber:

$$t_{RT}(z) = 2\int_0^z \frac{n(z)}{c}dz\,, \tag{1}$$

where $n(z)$ is the refractive index of the fiber, is accurately measured at the receiver and is used to map the contributions of $B(t)$ to the positions of the fiber that generates them. If the fiber is kept at rest, consecutive interrogations of the fiber will generate always the same trace. However, if a perturbation $\xi(t)$ acts section of the fiber $I = [z_i, z_j]$, the consequent refractive index variation $\Delta n(t)$ induces a local shift in $B(t)$, for all $t = t_{RT}(I)$. This can be seen in Fig. 1(a), where the exemplary simplified traces corresponding to a reference trace $B_r(t)$ and a stressed trace $B_s(t)$ collected respectively before and during the perturbation $\xi(t)$ are represented. As can be seen, around $t = 5\ \mu s$ the stressed trace, which at the beginning was perfectly overlapped with the reference, experiences a visible shift. In chirped pulse φ-OTDR setups, the measure is performed by dividing $B_r(t)$ and $B_s(t)$ into corresponding windows. For each couple of corresponding windows, a correlation operation is performed and the central peak is monitored. Due to the local shift induced by $\Delta \mathrm{n}(t)$ in $B_s(t)$,the correlation peak of the windows corresponding to the section I of the fiber will move of a value Δt:

$$\frac{\Delta \mathrm{n}(t)}{n} = -\left(\frac{1}{\upsilon_0}\right)\left(\frac{\delta \upsilon}{\tau_p}\right)\Delta t. \tag{2}$$

By inverting eq. (2) the value of $\Delta n(t)$, which is linearly proportional to the acting perturbation, can be extracted allowing the sensing of temperature changes or vibrations with extremely high sensitivities (in the order of mK or nε). Observing eq. (1), it is possible to see that the refractive index variation induced by the perturbation in I causes a change $\Delta t_{RT}(z)$ common to all the round trip times $t_{RT}(z)$ with $z > z_j$. All corresponding contributions of $B_s(t)$ will then experience a small, common shift, visible in Fig. 1(a) for $t > 7\ \mu s$, where even if no perturbation is acting, the two lines are not as perfectly overlapped as they were at the beginning. This common shift, due to eq. (2), will appear in the results as a small distributed virtual perturbation.

The theoretical model of this "virtual" perturbation is developed considering as stressing perturbation a uniform temperature change $\xi(t) = \Delta T(t)$ acting on a section I, of length $L = z_j - z_i$ of the fiber. When the section of the fiber I, supposed at room temperature, experiences a temperature change $\Delta T(t)$, the length of the fiber changes due to thermal expansion, $\tilde{L}(t) = L + \Delta L(t)$, and the local refractive index changes due to the thermo-optic effect, $\tilde{n}(t) = n + \Delta n(t)$. Knowing the silica linear thermal expansion coefficient[7], $\alpha \cong 0.55 \cdot 10^{-6}$ [°C^{-1}], and thermo-optic coefficient[8], $\zeta_T \cong 6.92 \cdot 10^{-6}$[°C^{-1}], the thermal expansion results $\Delta L(t) = \alpha \Delta T(t) L$ and the refractive index variation $\Delta n(t) = \zeta_T \Delta T(t) n$. The common change in the round trip times $\Delta t_{RT}(z)$ for all positions after I can then be expressed as:

$$\Delta t_{RT}(z) \ = 2\left[\int_0^{\tilde{L}(t)} \frac{\tilde{n}(t)}{c}dz - \int_0^{L} \frac{\mathrm{n}}{c}dz\right] = 2\frac{\tilde{n}(t)\tilde{L}(t)}{c} - 2\frac{nL}{c} \approx 2\frac{n\Delta L(t)}{c} + 2\frac{\mathrm{n}(t)L}{c} \tag{3}$$

where the term proportional to $\Delta L(t)\Delta \mathrm{n}(t)$ is ignored since it is many orders of magnitude lower than the others.

According to eq.(2), the $\Delta t_{RT}(z)$ reported in eq. (3) appears in the measurement as a virtual change of the refractive index, thus as a virtual temperature change $\delta T(t)$, according to

$$-\left(\frac{1}{\upsilon_0}\right)\left(\frac{\delta \upsilon}{\tau_p}\right)\Delta t_{RT}(z) = \frac{\Delta n_{RT}(t)}{n} = \zeta_T \delta T(t) \tag{4}$$

By substituting (3) in (4), and solving for $\delta T(t)$ we get:

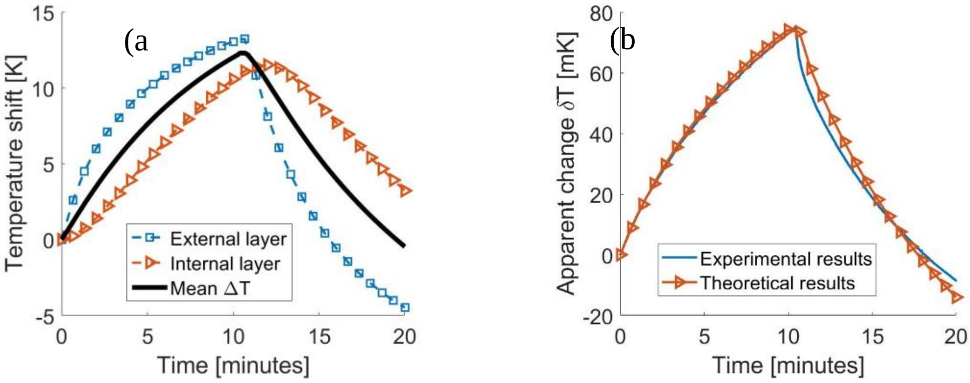

Figure 2. (a) Temperature changes in the stressed fiber measured in different positions (marked lines); Mean temperature change of the stressed fiber (solid line). (b) Measured virtual temperature change in the reference fiber (blue line) compared with the expected result (marked red line).

$$\delta T(t) = K\frac{1}{\zeta_T}\frac{1}{\upsilon_0}\frac{\delta\upsilon}{\tau_p}\left[\frac{2n\Delta L(t)}{c} + \frac{2\Delta \mathrm{n}(t)L}{c}\right] = K\frac{1}{\zeta_T}\frac{1}{\upsilon_0}\frac{\delta\upsilon}{\tau_p}\frac{2nL}{c}\left[\alpha\Delta T + \zeta_T\Delta T(t)\right] \tag{5}$$

where the first term is related only to the thermal expansion and the second only to the thermo-optic effect. The two terms differ only for the coefficients α and ζ_T, thus the contribution of the thermo-optic effect on $\delta T(t)$ is about one order of magnitude higher than the one induced by thermal expansion. A constant scaling factor K has been added in the model of eq. (5), because the actual values of the thermo-optic coefficient ζ_T and of the thermal expansion coefficient α of the fiber used may be different from the ones reported in the literature.

A similar model can be derived if the measured perturbation is translated into strain reading $\Delta\varepsilon(t)$ instead of a temperature change. In such a case the apparent strain may be derived as:

$$\delta\varepsilon(t) = K\frac{1}{\zeta_\varepsilon}\frac{1}{\upsilon_0}\frac{\delta\upsilon}{\tau_p}\frac{2\Delta \mathrm{n}(t)L}{c} \tag{6}$$

where[8] $\zeta_\varepsilon = 0.78$ is the elasto-optic coefficient for germanium-doped silica-core fiber and $\Delta\mathrm{n}(t)$=$\zeta_\varepsilon\Delta\varepsilon(t)n$ is the change in the fiber refractive index caused by the strain due to the elasto-optic effect.

3. EXPERIMENTAL SETUP AND RESULTS

The setup used to validate the proposed model is schematically represented in Fig. 1(b). A link of standard SMF-28 fiber of total length $L = 18.9\,km$, made of three different sections called respectively launch, stressed and reference, is connected to a standard chirped pulse φ-OTDR[4]. The laser source at $\lambda_0 = 1550\,nm$ generates chirped pulses of width $\tau_p = 100\,ns$ and total chirp of $\delta\upsilon = 1\,GHz$. The launch fiber is $L_L = 0.9\,km$ long and it is used to estimate and correct, in post-processing, the laser phase-noise on the other fiber sections[9]. The temperature change $\Delta T(t)$ is induced on the stressed fiber, which is $L_S = 16.6\,km$ long, by submerging it with water at different temperatures. Finally the reference fiber, which is $L_S = 1.4\,km$ long, is used to measure the virtual temperature change $\delta T(t)$ induced by $\Delta T(t)$ on L_S. As can be seen in Fig. 1(b), the launch and the reference fibers are immersed into room temperature water, represented by a light blue color, to partially isolate them from undesired environmental perturbations. To avoid the floating of the coils, a weight was placed on their top, anchoring them to the bottom of the bucket.

The measurement started by submerging L_S in water at a temperature $T_H = 15\,K$ higher than the room temperature. To allow a sufficient thermalization, the setup was left measuring unperturbed for the successive 10 minutes before changing the warm water with cold one at a temperature $T_C = 8\,K$ lower than the room temperature for 10 more minutes. The amount of water poured in both cases is sufficient to consider the water's temperature as a constant during the thermalization process. Due to the fiber low thermal conductivity, the temperature change induced by the water on different layers of the stressed coil is not uniform and the chirped pulse φ-OTDR measures, along L_S, a position-depending perturbations $\Delta T(t, z)$. This is clearly visible in Fig. 2(a) where the temperature changes measured at an outer (blue line, square marker) and inner (red line, triangular marker) layers, are represented. As can be seen, during the whole measurement the temperature of the layer closer to the water shows a fast exponential-like response, in agreement with the Newtonian laws of warming/cooling, while the inner layer shows a delayed and almost linear change. Thanks to the linearity of the phenomena involved in the experiment, it is convenient to average all the position-dependent terms $\Delta T(t,z)$ into an equivalent uniform temperature change $\Delta T(t)$, reported in Fig. 2(a) as a black solid line.

Due to instrument-related noise and remaining undesired environmental stresses, the measurements $\delta T(t,z)$ acquired in the reference fiber represent position-dependent noisy replicas of the virtual perturbation $\delta T(t)$, which can be averaged along the position axis. The result is shown in Fig. 2(b) where, with respect to the left vertical axis, the experimental (blue line) and expected (marked red line) curves are plotted. The expected curve was computed from the model in eq. (5), using as parameters $K = 0.78$, $\Delta L = L_S$ and the equivalent uniform temperature change $\Delta T(t)$. As can be seen, there is a great agreement between the curves, even if a slight mismatch is visible during the cool-down. This difference is probably the consequence of the strains induced on the fiber during the water exchange phase, which distort the received backscattering trace $B(z)$ reducing the quality of the correlation operation used to perform the measurement, thus increasing the noise.

4. CONCLUSION

In this paper we have proposed a theoretical model representing the virtual perturbation introduced in the chirped pulse φ-OTDR measurement, by a real perturbation acting on a previous section of the fiber. An experiment has been performed to validate the model, obtaining results in great agreement with the theoretical prediction. The model can be used to estimate and progressively correct the errors introduced thus improving the quality of the measurement performed with chirped pulse φ-OTDR, especially for weak perturbations.

ACKNOWLEDGMENT

This work was supported by project FINESSE MSCA-ITN-ETN-722509; the DOMINO Water JPI project under the WaterWorks2014 cofounded call by EC Horizon 2020, the Spanish MINECO and Italian MIUR; Comunidad de Madrid and FEDER Program (P2018/NMT-4326); project TEC2015-71127-C2-2-R, RTI2018-097957-B-C31, HFM acknowledges financial support from the Spanish Ministery (MICINN) under contract no. IJCI-2017-33856, respectively. LM acknowledge Fondazione Ing. Aldo Gini for partial financial support, AGR.University of Alcalá (FPI).

REFERENCES

[1] Bao, X., and Chen, L., “Recent Progress in Distributed Fiber Optic Sensors,” Sensors., 12(7), 8601–8639 (2012)

[2] Bucaro, J. A., and Hickman, T. R., “Measurement of sensitivity of optical fibers for acoustic detection,” Appl. Opt., 18(6), 938 (1979).

[3] Juarez, J. C. , Maier, E. W., Choi, K. N., and Taylor, H. F., “Distributed fiber-optic intrusion sensor system,” J. Light. Technol., 23(6), 2081–2087 (2005).

[4] Pastor-Graells, J., Martins, H. F., Garcia-Ruiz, A., Martin-Lopez, S., and Gonzalez-Herráez, M., “Single-shot distributed temperature and strain tracking using direct detection phase-sensitive OTDR with chirped pulses,” Opt. Express, 24(12), 13121 (2016).

[5] Juarez, J. C. , and Taylor, H. F., “Field test of a distributed fiber-optic intrusion sensor system for long perimeters,” Appl. Opt., 46(11), 1968 (2007).

[6] Peng, F., Wu, H., Jia, X.-H., Rao, Y.-J., Wang, Z.-N., and Peng, Z.-P., “Ultra-long high-sensitivity Φ-OTDR for high spatial resolution intrusion detection of pipelines,” Opt. Express, 22(11), 13804–13810 (2014).

[7] White, G. K., “Thermal expansion of reference materials: copper, silica and silicon,” J. Phys. D, 6(17), 2070–2078 (1973).

[8] Koyamada, Y., Imahama, M., Kubota, K., and Hogari, K., “Fiber-Optic Distributed Strain and Temperature Sensing With Very High Measurand Resolution Over Long Range Using Coherent OTDR,” J. Light. Technol., 27(9), 1142–1146 (2009).

[9] Fernández-Ruiz, M. R., Pastor-Graells, J., Martins H. F., García-Ruiz, A., Martín-López and M. González-Herráez, “Laser Phase-Noise Cancellation in Chirped-Pulse Distributed Acoustic Sensors,” J. Light. Technol., 36(4), 975–985 (2018).